

GEOOTHERMAL RESERVOIR SIMULATIONS WITH SHAFT79

by Karsten Pruess and Ron C. Schroeder

Lawrence Berkeley Laboratory, Berkeley, Ca. 94720

INTRODUCTION

The rational development of geothermal resources requires an adequate knowledge of the behavior of a given reservoir under various production and injection schemes. Mathematical modeling attempts to provide such knowledge and to determine important reservoir parameters, such as formation permeabilities and reserves of fluid and heat.

Because of phase changes and because of the coupling between energy- and mass-flow, the equations describing geothermal reservoirs are strongly non-linear. This limits the applicability of analytical approximations and has motivated the development of numerical simulators. In this paper, we review the concepts and methods used in LBL's geothermal simulator SHAFT79, and illustrate its application to a variety of typical problems.

PHYSICAL MODEL AND SOLUTION METHOD

The simulator SHAFT79 was developed for computing two-phase flow phenomena in geothermal reservoirs. The program handles transient initial-value problems with prescribed boundary conditions. SHAFT79 is an improved version of the simulator SHAFT78, which was discussed in detail in ref. 1). It solves coupled equations for mass- and energy-transport, using an integrated finite difference method. This method allows a very flexible description of reservoirs because it does not distinguish between one-, two-, or three-dimensional regular or irregular geometries.

The main assumptions and approximations made in the formulation of SHAFT79 are as follows:

(1) Geothermal reservoirs are approximated as systems of porous rock saturated with one-component fluid in liquid and vapor form. (2) All rock properties - porosity, density, specific heat, thermal conductivity, absolute permeability - are independent of temperature, pressure, or vapor saturation. (3) Liquid, vapor, and rock matrix are in local thermodynamic equilibrium,

i.e. at the same temperature and pressure, at all times. (4) Capillary pressure is neglected.

The main new feature in SHAFT79 as compared with SHAFT78 is a completely simultaneous, iterative solution of the coupled mass- and energy-transport equations. This allows between ten and one hundred times larger time steps than the sequential method employed in SHAFT78. In particular, phase transitions can be computed accurately and efficiently. SHAFT79 offers a choice of several methods for solving the coupled non-linear equations for mass- and energy-flow. The preferred solution method is fully implicit, employs a Newton/Raphson iteration for simultaneous solution of the non-linear mass- and energy-transport equations, and uses an efficient sparse solver.²⁾ SHAFT79 has been applied to problems with up to 350 elements in three dimensions. Typical throughputs range from 0.1 in highly transient situations to more than 10^6 in problems approaching steady state. Here throughput is defined as ratio of the fluid mass flowing through the surface of an element in one time step, divided by the fluid mass initially in place in that element.

APPLICATIONS

Table 1 gives an overview of the types of systems and processes which have been modeled with SHAFT79. Below are presented results of selected SHAFT79-simulations which illustrate the range of applications. Parameters for the individual cases are given in the figure captions. Relative permeabilities were obtained from Corey's equations, with residual immobile steam saturation S_{sc} equal to zero, and residual immobile water saturation S_{wc} varying between 0.40 and 0.70.

DEPLETION OF A RESERVOIR WITH SHARP STEAM/WATER INTERFACE

When steam is produced from above a liquid water table, boiling commences near the top of the water zone. This gives rise to a drop in temperature and pressure, whereby a two-phase layer between water and steam zones is established. Water moves upward into the two-phase zone, releasing pressure below the boiling front and advancing it downward.³⁾ In

GEOMETRY	TYPE OF PROBLEM	SIMULATED PROCESSES
1-D, rectangular	depletion of two-phase geothermal reservoirs ³⁾	various production and injection schemes for reservoirs with uniform initial conditions or with sharp steam/water interfaces
1-D, cylindrical	two-phase flow near wells	production from two-phase zones; cold water injection into two-phase and superheated steam zones, respectively
2-D, rectangular	Krafla geothermal reservoir (Iceland) ⁴⁾	different space and time patterns of production and injection
2-D, cylindrical	high level nuclear waste repository ⁵⁾	long-term evolution of temperatures and pressures near a powerful heat source (in progress)
3-D, regular	two-phase interference test in Cerro Prieto (Mexico)	(in progress)
3-D, irregular	Serrazzano geothermal reservoir (Italy) ³⁾	detailed field production from 1960 to 1966

Table 1: Simulation Studies with SHAFT79.

the examples studied (see fig. 1) the top of the two-phase zone does not dry up until after the boiling front has reached the bottom of the reservoir. This occurs after 6.4 years for the "high permeability" case (A in fig. 1), and after 9.6 years for the "low permeability" case (B in fig. 1). Vapor saturation at the top of the water table then reaches 46.7 % for case A and 78.9 % for case B. Pressure at the steam/two-phase interface, at a depth of 500 m, declines very slowly during the advancing of the boiling front in case A. The reason for this is that the most rapid boiling occurs at the bottom of the two-phase zone. This provides a supply of hotter steam, which flows up from depth and tends to maintain temperature and hence pressure at the top of the two-phase zone. In case B this mechanism for pressure maintenance is much less effective because of the lower permeability.

INJECTION OF COLD WATER

Cold water injection into a steam reservoir gives rise to a hydrodynamic front and, trailing behind it, a temperature front. In the finite-difference simulation of this process subsequent elements undergo phase transitions from superheated steam

to two-phase conditions to subcooled water. Fig. 2 shows the fronts at two different times. It is apparent that the fronts are propagated according to the parameter t/R^2 . The volume swept by the temperature front is close to 1/4 of the volume swept by the hydrodynamic front. This reflects the fact that, at a porosity of 20 %, the volumetric heat capacity of water is about 1/4 of the volumetric heat capacity of the rock/water mixture.

SIMULATION OF KRAFLA FIELD (ICELAND)

Fig. 3 shows a vertical two-dimensional grid as used by Jonsson for simulating production and injection at Krafla.⁴⁾ The reservoir is initially almost entirely filled with liquid water close to saturated conditions. Various production and injection schemes were explored in an attempt to optimize injection, i.e. to combine pressure and temperature maintenance during production with minimal sacrifices in terms of decreasing vapor saturation S. Fig. 4 shows typical results. Jonsson finds that deep injection is preferable to shallow injection. Complete problem specifications and discussions of results are given in ref. 4).

SIMULATION OF SERRAZZANO FIELD (ITALY)

The most complex simulation effort undertaken with SHAFT79 to date is a case study (history match) of the Serrazzano reservoir. Serrazzano is one of the distinct zones of the extensive geothermal area near Larderello in central Tuscany (Italy).

Detailed production data gathered since 1939 and an extensive body of geological and hydrological work make Serrazzano an attractive example for developing geothermal reservoir simulation methodology (see references given in 3). Fig. 5 gives a map of the reservoir, and fig. 6 shows the geologically accurate mesh as developed by Weres.⁷⁾ Conceptual model of the reservoir and parametrization of the problem are discussed in refs. 3) and 7).

Many parameters are only partially known, and are determined in trial-and-error fashion by comparing simulated reservoir performance with field observations. A valuable criterion for determining absolute permeabilities is that well blocks must remain very close to steady flow conditions. Our most complete simulation so far covers the period from 1960 to 1966. With the permeability distribution as indicated in fig. 5 we achieve steady flow for all wells producing since 1961 or earlier to within 2 % for the entire six year period modeled (i.e., the difference between inflow and production for any well block never exceeds 2 %).

From mass balance considerations it can be shown that most of the fluid reserves in Serrazzano are in place in liquid form. Little is known, however, about the distribution of pore water in the reservoir. Making the tentative assumption that liquid water is distributed throughout most of the reservoir, we compute a pressure decline (see fig. 7) which is slower than observed in the field by a factor of approximately 3.5. In the simulation pressure declines slowly because boiling is spread out over a large volume. We conclude that in most of the reservoir volume no liquid water is present, and we shall modify our initial conditions accordingly in subsequent simulations. We also need to correct some imbalances in initial conditions, which are apparent from the initial non-monotonic behavior of pressure in fig. 7.

CONCLUSION

The simulator SHAFT79 uses efficient methods for computing mass- and energy-transport in geothermal reservoirs, and allows for a flexible description of irregular geometric features. A broad range of applications, including idealized systems as well as large field problems, demonstrates its usefulness for geothermal reservoir studies. Further development work is presently under way to improve on some of the restrictive approximations made in the formulation of the physical model.

ACKNOWLEDGEMENT

This work was supported by the U.S. Department of Energy under contract No. W-7405-ENG-48.

REFERENCES

- (1) K. Pruess, J.M. Zerzan, R.C. Schroeder, and P.A. Witherspoon, Description of the three-dimensional two-phase simulator SHAFT78 for use in geothermal reservoir studies, paper SPE-7699, presented at the Fifth Symposium on Reservoir Simulation, Denver/Colorado, 1979.
- (2) I.S. Duff, MA28 - a set of Fortran subroutines for sparse unsymmetric linear equations, Report AERE - R 8730, Harwell/Oxfordshire, Great Britain (June 1977).
- (3) K. Pruess, G. Bodvarsson, R.C. Schroeder, P.A. Witherspoon, R. Marconcini, G. Neri, and C. Ruffilli, Simulation of the depletion of two-phase geothermal reservoirs, paper SPE-8266, presented at the 54th Annual Fall Technical Conference and Exhibition of the SPE, Las Vegas/Nevada, 1979.
- (4) V. Jonsson, Lawrence Berkeley Laboratory Report LBL-10003 (in preparation).
- (5) R. Eaton, private communication.
- (6) S.K. Garg, Pressure transient analysis for two-phase (liquid water/steam) geothermal reservoirs, paper SPE-7479, presented at the 53rd Annual Fall Technical Conference and Exhibition of the SPE, Houston/Texas, 1978.
- (7) O. Weres, A model of the Serrazzano zone, Proc. Third Stanford Workshop on Geothermal Reservoir Engineering, Stanford/California, 1977.

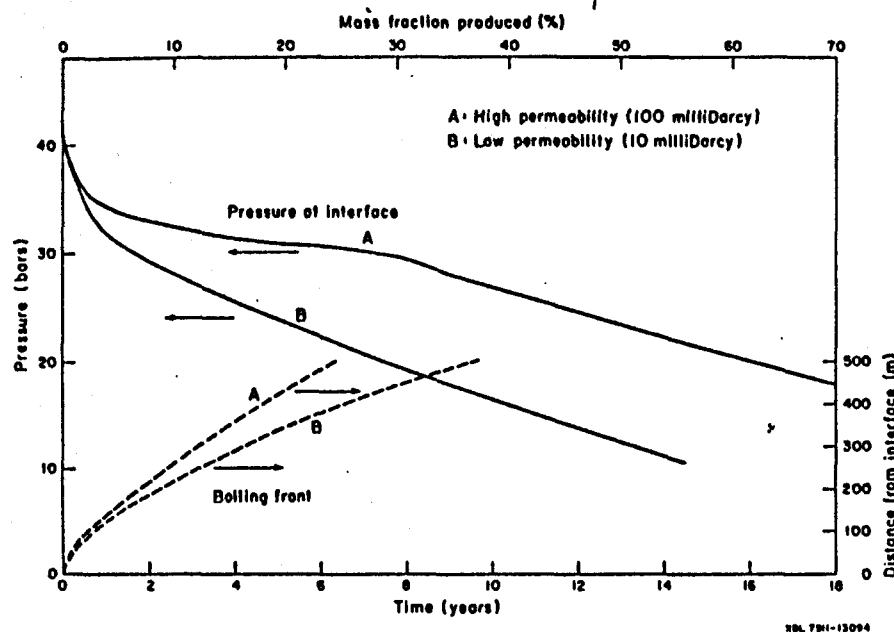


Fig. 1: Depletion of a reservoir with sharp steam/water interface. The reservoir is a vertical column of 1 km depth with a volume of 1 km^3 and "no flow" boundaries. For purposes of numerical simulation it is subdivided into 44 horizontal elements. Initially, the bottom half is filled with liquid water, the top half with superheated steam, with temperature $T = 252^\circ\text{C}$ and pressures carefully equilibrated under gravity. (Rock parameters: density = 2000 kg/m^3 ; specific heat = $1232 \text{ J/kg}^\circ\text{C}$; porosity = 10 %; residual immobile water saturation = 70 %) Depletion occurs uniformly at the top with a constant rate of 50 kg/s . The curves are for a permeability of 10^{-13} m^2 (A) and 10^{-14} m^2 (B), respectively. Typical time steps in the simulation are $2 - 5 \times 10^6$ seconds, corresponding to throughputs of up to 250.

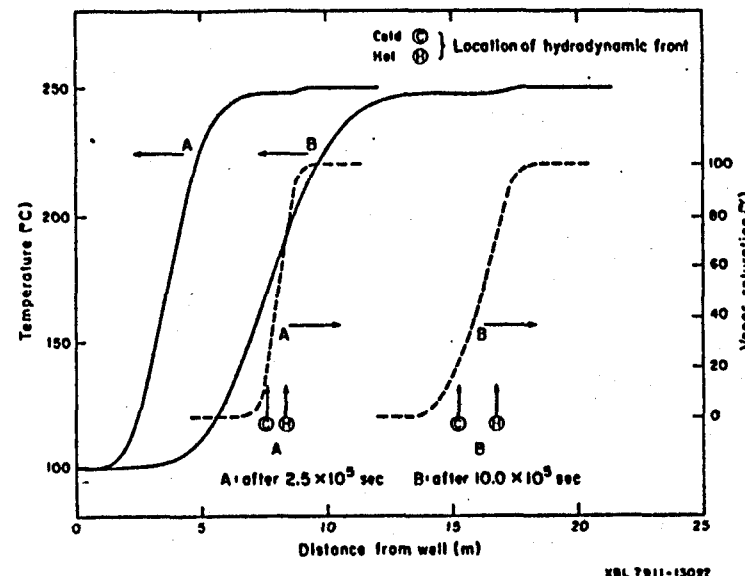


Fig. 2: Injection of cold water into a steam zone. The reservoir is a cylinder with large radius, initially filled with superheated steam at $T = 250^\circ\text{C}$, pressure = 38 bars. Water with $T = 99.3^\circ\text{C}$ is injected along the center line at a constant rate of 0.14 kg/s m . The numerical simulation employs an axisymmetric grid as used by Garg.⁶⁾ (Rock parameters: density = 2650 kg/m^3 ; specific heat = $1000 \text{ J/kg}^\circ\text{C}$; porosity = 20 %; heat conductivity = $5.25 \text{ W/m}^\circ\text{C}$; permeability = 10^{-13} m^2 ; residual immobile water saturation = 40 %) The simulation uses time steps from 2500 to 10000 seconds, with throughputs of up to 6. The arrows labeled C and H show the locations of the hydrodynamic front if all injected water were to remain at injection temperature (C) or were heated up to initial reservoir temperature (H).

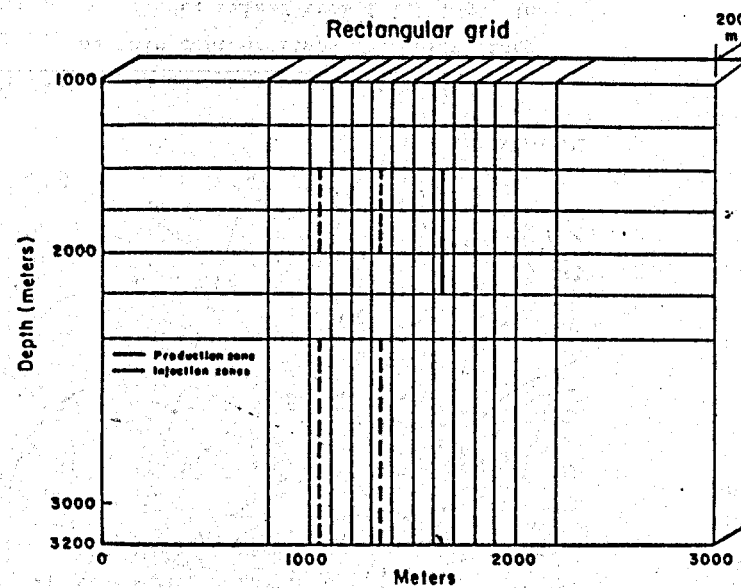


Fig. 3: Two-dimensional grid for simulation of Krafla (Iceland). (from ref. 4)

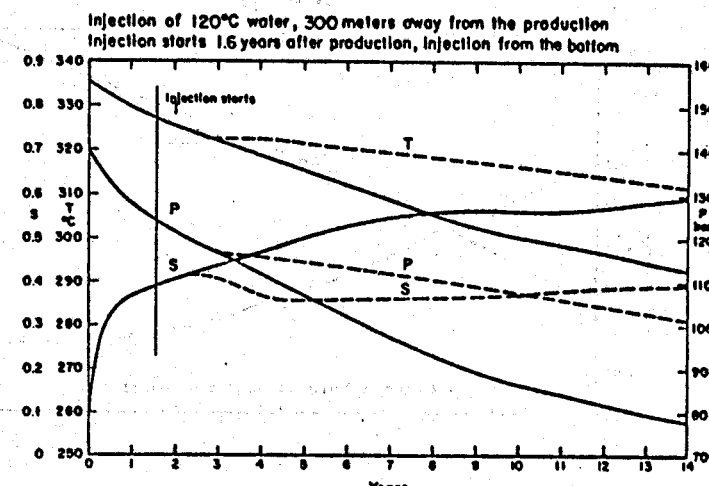


Fig. 4: Simulated performance of Krafla reservoir.

Temperature, pressure and vapor saturation at the well block are given as function of time with injection (dashed lines) and without injection (solid lines). Production rate is 45 kg/s and injection rate is 22.5 kg/s. Typical time steps in the simulation are 1.25×10^6 seconds, with throughputs of about 0.1 (from ref. 4).

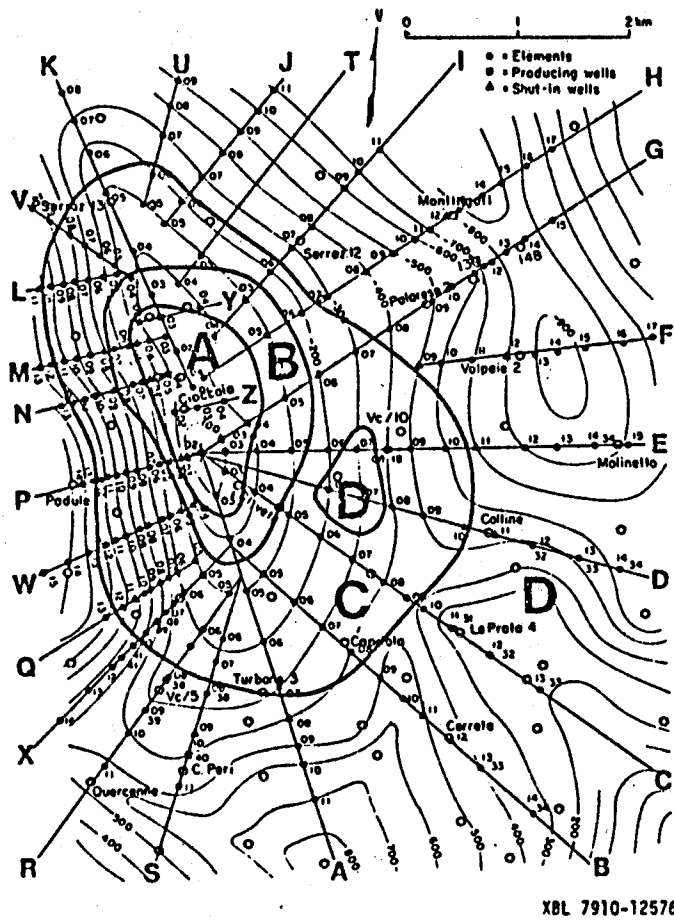


Fig. 5: Aerial map of Serrazzano geothermal reservoir. The thin contour lines show elevations of the cap rock as determined from drill logs. The straight lines labeled A to Z indicate the locations of geological cross sections used in constructing a three-dimensional finite difference grid.⁷⁾ Locations of elements (nodes) are also shown. A - D are regions of different permeability as determined in the simulation: A - $0.75 \times 10^{-12} \text{ m}^2$; B - $0.25 \times 10^{-12} \text{ m}^2$; C - $0.75 \times 10^{-13} \text{ m}^2$; D - $0.15 \times 10^{-13} \text{ m}^2$.

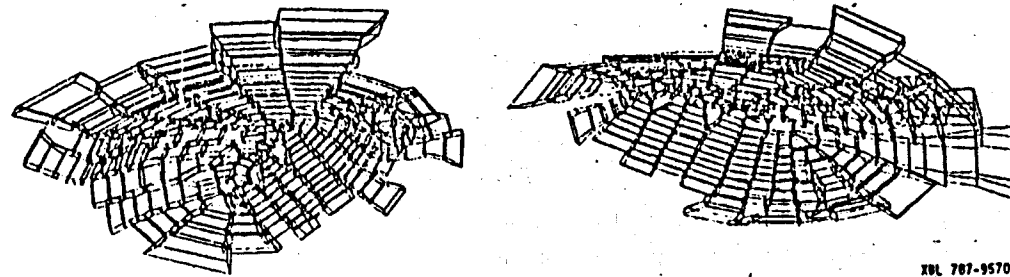


Fig. 6: Serrazzano grid. The computer-generated geologically accurate grid of the Serrazzano reservoir as developed by Weres is shown in two rotated perspective views (ref. 7). This three-dimensional grid represents a reservoir that is a curved thin sheet approximately 1 km from top to bottom, with an aerial extension of about 25 km^2 . It has 234 polyhedral elements, with 679 polygonal interfaces between them. There are up to 10 interfaces per element.

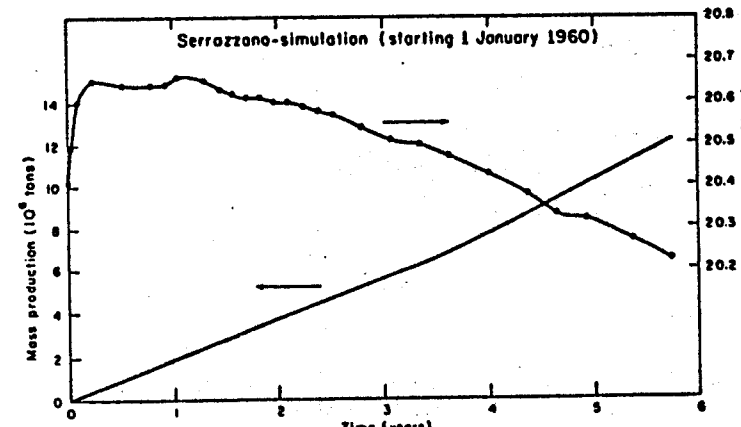


Fig. 7: Average reservoir steam pressure and cumulative fluid production as calculated in Serrazzano simulation. Typical time steps in the simulation are 10 to 50 days, with throughputs of up to 65.